RF Circuits and Systems, M.Tech CS - I

Mini Project Report

On

10-Element Yagi Antenna For 38 GHz Frequency

Submitted by

Bhavya Desai

(P25EC005)

Guided by

Mahesh Hasani

Research Scholar, ECED-SVNIT

&

Dr. Kirti Inamdar

Assistant Professor, ECED-SVNIT

DEPARTMENT OF ELECTRONICS ENGINEERING

SARDAR VALLABHBHAI NATIONAL INSTITUTE OF TECHNOLOGY

DECEMBER 2025

Abstract

The design and analysis of a 10-element Yagi–Uda antenna operating at 38 GHz are presented in this report. The antenna was reconstructed in CST Studio Suite based on the specifications provided in a reference research paper, with all element lengths and spacings derived from wavelength-scaled calculations. The implemented model was simulated to evaluate key performance metrics including return loss, gain, surface current distribution, and radiation characteristics. The antenna achieved a return loss of -16.08 dB at the target frequency, along with a peak gain of 10.8 dBi and a half-power beamwidth of approximately $52°$, confirming strong end-fire radiation. The 2D and 3D far-field patterns further validate proper coupling between the reflector, driven element, and director array. A comparison with the reference work shows close agreement across all major parameters, demonstrating that the reproduced design accurately achieves the intended millimeter-wave performance.

1 Introduction

Millimeter-wave communication has become a key enabler for emerging high-capacity wireless systems, particularly in fifth-generation (5G) networks where large bandwidths are available at higher frequencies. Operating in the 38 GHz band demands antenna structures that can overcome high propagation losses and provide strong directional gain. Among various compact end-fire radiators, the Yagi–Uda antenna stands out for its simple geometry, ease of fabrication, and ability to deliver high directivity with a low profile. Its combination of a reflector, driven element, and multiple directors makes it highly efficient for point-to-point links and long-distance transmission, which are common requirements in modern millimeter-wave systems. The design simulated in this report is based on the 10-element Yagi array proposed in the referenced work, which demonstrates notable performance including a return loss of –16.08 dB and a peak gain of 10.8 dB at 38 GHz.

Yagi antennas have traditionally been used in ISM-band applications such as 2.4 GHz wireless links, industrial sensing, and scientific instrumentation, where directional radiation and high front-to-back ratio are essential. Their advantages—high gain, narrow beamwidth, and simple physical structure—extend naturally into millimeter-wave domains, enabling use cases in 5G base stations, short-range backhaul, automotive radar, high-data-rate short-range links, and compact RF front-ends. Recent research also explores filtered and planar Yagi configurations that integrate multiple RF functions to reduce device size and enhance system efficiency, reflecting the broader trend toward miniaturized high-performance antennas.

In this work, the 10-element Yagi model from the paper is reproduced and simulated using CST Studio Suite, a full-wave electromagnetic simulation software widely used for high-frequency antenna design and optimization. The paper provides element dimensions derived from wavelength-based scaling, with the reflector, driven element, and directors optimized for the 38 GHz operating band. These parameters guide the reconstruction of the antenna in CST, and the resulting simulations allow evaluation of key performance metrics such as S-parameters, surface current distribution, radiation characteristics, and overall antenna efficiency, forming the basis for the results presented in later chapters.

2 Antenna Theory and Design

2.1 Yagi–Uda Antenna Theory

The Yagi–Uda antenna is a widely used end-fire radiating structure known for its high directivity, compact form, and simple construction. It consists of one driven element and several parasitic elements whose mutual coupling shapes the radiation pattern. The interaction of induced currents on these elements produces constructive interference in the forward direction and destructive interference toward the rear, enabling strong unidirectional radiation. Such characteristics make Yagi antennas highly suitable for point-to-point and long-range wireless links, especially in the millimeter-wave region where signal attenuation is significant and high-gain, narrow-beam antennas are essential for reliable communication. Figure 2.1 shows a general structure of Yagi-Uda Antenna.

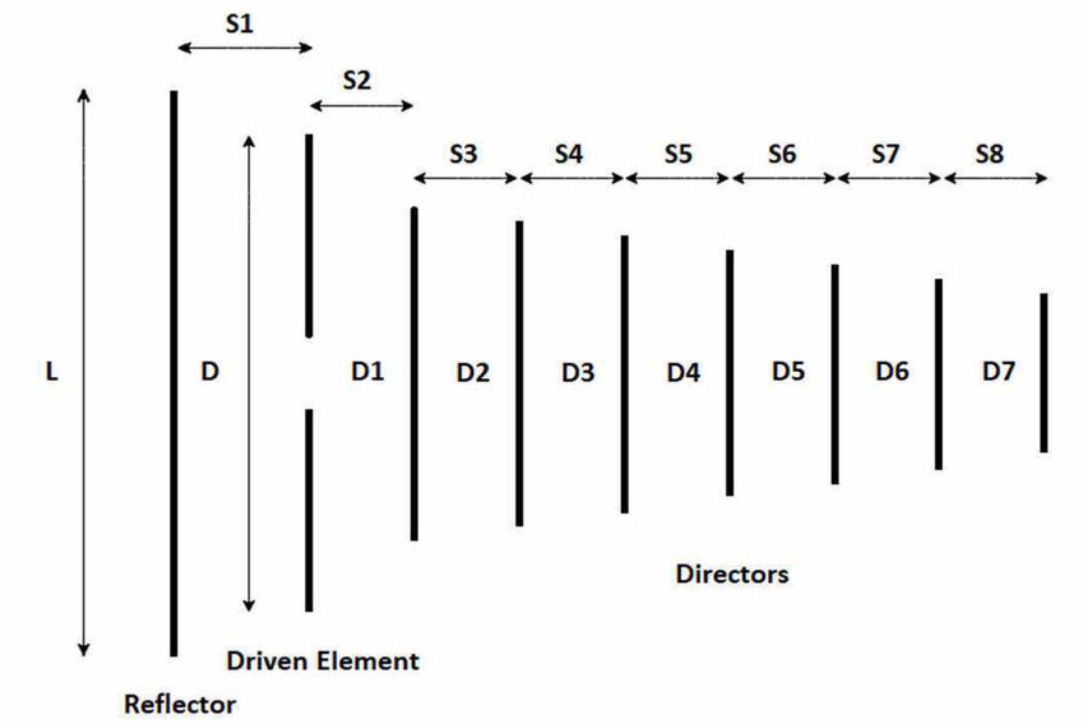

Figure 2.1: Implemented Yagi–Uda antenna model in CST Studio Suite.

2.1.1 Elements of a Yagi–Uda Antenna

- **Driven Element:** Typically a half-wavelength dipole that is directly excited by the feed.
- **Reflector:** Slightly longer than the driven element; positioned behind it to suppress backward radiation.

- **Directors:** A set of parasitic elements in front of the driven element; each slightly shorter than the previous one to enhance forward radiation.

2.1.2 Operating Principle

The operation of a Yagi–Uda antenna is governed by the interaction between its driven element and the surrounding parasitic elements. When the driven element is excited, it generates an electromagnetic field that induces currents on both the reflector and the directors. These parasitic elements then re-radiate energy with phase shifts determined by their physical dimensions and spacing. The reflector, being slightly longer, introduces a phase lag that suppresses radiation toward the rear, while the shorter directors create a phase lead that strengthens radiation in the forward direction. Together, these effects produce constructive interference along the end-fire axis of the antenna, resulting in a focused, high-gain beam. This coordinated electromagnetic behavior gives the Yagi–Uda antenna its well-known characteristics of high directivity, narrow beamwidth, and efficient unidirectional radiation—features that are especially valuable in long-range and millimeter-wave communication systems.

The dimensions of each element in a Yagi–Uda antenna are selected as specific fractions of the operating wavelength (λ) because resonant behavior and induced currents depend strongly on how each element relates to the wavelength. A half-wavelength conductor naturally supports a strong standing wave, making it ideal for the driven element. The reflector is made slightly longer than $\lambda/2$ to introduce the required phase delay for effective back-lobe suppression. In contrast, the directors are progressively shorter, which advances their phase and helps pull the radiated energy forward, improving gain and maintaining an end-fire pattern. Expressing the inter-element spacing in terms of λ ensures proper electromagnetic coupling, allowing the fields from all elements to combine coherently. The table 2.1 summarizes the specific element lengths and spacings used in the Yagi–Uda antenna design.

Table 2.1: Design Specifications of the Yagi–Uda Antenna

Element	**Specification (in λ)**
Length of the Driven Element	0.458 – 0.50
Length of the Reflector	0.55 – 0.58
Length of Director 1	0.45
Length of Director 2	0.40
Length of Director 3 onwards	0.35
Spacing Between Directors	0.20
Reflector to Dipole Spacing	0.35
Dipole to Director Spacing	0.125

2.2 Design Specifications and Element Calculations

The Yagi–Uda antenna implemented in this work follows the design parameters reported in the reference paper, targeting an operating frequency of 38 GHz for millimeter-wave applications. At such high frequencies, element dimensions must be chosen with high precision because even small deviations can shift the resonant frequency or alter the radiation characteristics. The specification values are derived as fractions of the wavelength, ensuring proper phase relationships and efficient end-fire radiation.

2.2.1 Operating Frequency and Wavelength

The free-space wavelength corresponding to the 38 GHz operating frequency is calculated using

$$\lambda = \frac{c}{f}, \tag{2.1}$$

where $c = 3 \times 10^8$ m/s is the speed of light and $f = 38 \times 10^9$ Hz. Thus,

$$\lambda = 7.89\,\text{mm}. \tag{2.2}$$

All element lengths and spacings are determined as fractions of this wavelength to maintain accurate phase alignment between the driven and parasitic elements.

2.2.2 Element Length Calculations

Using the wavelength value and specified dimensions of Yagi antenna given in table 2.1, the physical lengths of each element are computed as

$$L_{\text{element}} = k\lambda, \tag{2.3}$$

where k is the fractional multiplier taken from Table 2.1. For example, the driven element length is

$$L_{\text{driven}} = 0.5\lambda = 0.5 \times 7.89\,\text{mm} = 3.945\,\text{mm}. \tag{2.4}$$

Similarly, the spacing between the driven element and Director 1 is

$$S_{\text{dipole–director}} = 0.125\lambda = 0.125 \times 7.89\,\text{mm} = 0.986\,\text{mm}. \tag{2.5}$$

Each dimension of antenna can be calculated like shown above. The paper also optimizes these values through trial and error method, providing more accurate results. Table **??** compares theoretical values and optimized values for antenna implementation.

Table 2.2: Theoretical and Optimized Dimensions of the Yagi–Uda Antenna (All Dimensions in mm)

Element	Theoretical Value	Optimized Value (mm)
Length of Reflector	0.55λ	4.34
Length of Driven Element	0.50λ	3.94
Length of Director 1	0.45λ	3.55
Length of Director 2	0.40λ	3.15
Length of Director 3 onwards	0.35λ	2.76
Spacing Between Directors	0.2λ	1.58
Reflector to Dipole Spacing	0.35λ	2.76
Dipole to Director Spacing	0.125λ	0.99
Diameter of wire	0.2(mm)	0.2
Length of Discrete Port	0.4(mm)	0.4

2.3 Final Antenna Geometry and CST Implementation

All computed dimensions were used to construct the 10-element Yagi–Uda antenna model within CST Studio Suite. Each wire element was created using cylindrical coordinates, with the cylinder orientation aligned along the Z-axis so that every antenna element extends symmetrically above and below its midpoint. Diameter of 0.2 mm was selected for each wire element. Perfect Electric Conductor (PEC) material was assigned to all cylindrical elements, consistent with the reference design and ensuring minimal ohmic loss at millimeter-wave frequencies. The required spacing between elements was implemented precisely using their calculated X-coordinates, while the Y-coordinate was kept fixed at zero for all wires. A 50 Ω discrete port is applied at the center of the driven element to excite the structure. These dimensions and material settings collectively form the exact geometry used to generate the results presented in Chapter 3.

2.3.1 Co-ordinates calculations

The coordinate system is defined such that the midpoint of the driven element is placed at the origin, i.e. at

$$(0, 0, 0).$$

All parasitic elements are positioned with respect to this reference point. Since Director 3 is oriented along the z-axis, its length is divided equally about the origin of its own local axis. The total physical length of Director 3 is

$$L_{\text{Director3}} = 2.76 \text{ mm}.$$

Therefore, the element extends from

$$Z_{\text{min}} = -\frac{L_{\text{Director3}}}{2}, \qquad Z_{\text{max}} = +\frac{L_{\text{Director3}}}{2}.$$

Substituting the value:

$$Z_{\text{min}} = -\frac{2.76}{2} = -1.38 \text{ mm}, \qquad Z_{\text{max}} = +1.38 \text{ mm}.$$

The x-location of Director 3 is computed by adding the reflector–dipole spacing and the cumulative dipole–director spacings. Using:

$$S_{\text{Ref–Dipole}} = 0.35\lambda = 2.76 \text{ mm},$$

$$S_{\text{Dipole–Director}} = 0.125\lambda = 0.986 \text{ mm},$$

the x-coordinate of Director 3 is

$$X_{\text{Director3}} = S_{\text{Ref–Dipole}} + 3 \times S_{\text{Dipole–Director}}.$$

Substituting the numerical values:

$$X_{\text{Director3}} = 2.76 + 3(0.986) = 2.76 + 2.958 = 5.718 \text{ mm}.$$

Thus the final coordinates and height definition for Director 3 are:

$$X = 5.718 \text{ mm}, \qquad Y = 0,$$

$$Z_{\text{min}} = -1.38 \text{ mm}, \qquad Z_{\text{max}} = +1.38 \text{ mm}.$$

Table 2.3 shows all co-ordinates required for each element in form of X,Y,Zmin,Zmzx.

Table 2.3: Coordinates (X, Y, Z_{min}, Z_{max}) of Yagi–Uda Elements (mm)

Element	**X (mm)**	**Y (mm)**	**Z_{min} (mm)**	**Z_{max} (mm)**
Reflector	-2.7615	0.000	-2.1700	+2.1700
Driven element (midpoint)	0.0000	0.000	-1.9700	+1.9700
Discrete port	0.0000	0.000	-0.2000	+0.2000
Director 1	+0.9863	0.000	-1.7750	+1.7750
Director 2	+2.5643	0.000	-1.5750	+1.5750
Director 3	+4.1423	0.000	-1.3800	+1.3800
Director 4	+5.7203	0.000	-1.3808	+1.3808
Director 5	+7.2983	0.000	-1.3808	+1.3808
Director 6	+8.8763	0.000	-1.3808	+1.3808
Director 7	+10.4543	0.000	-1.3808	+1.3808

2.3.2 CST Implementation

Figure 2.2 shows the implemented 10-element Yagi–Uda antenna in CST Studio Suite.

A 50 Ω discrete face port was placed at the center of the driven element, with a port length of 0.4 mm, to provide excitation for the antenna model.

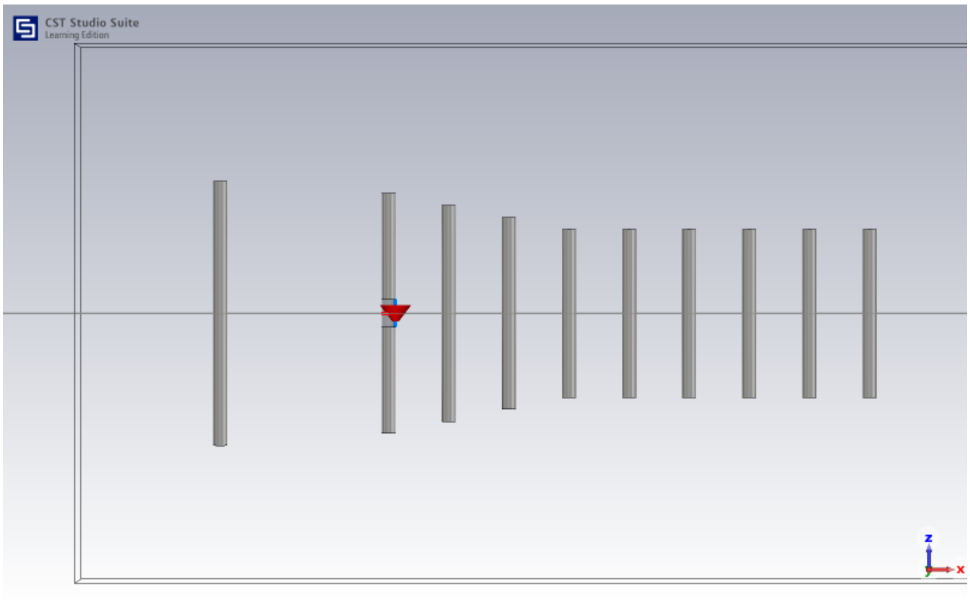

Figure 2.2: Implemented Yagi–Uda antenna model in CST Studio Suite.

3 Results and Discussion

This chapter presents the simulation results obtained from the CST model of the 10-element Yagi–Uda antenna. The results include the return loss characteristics, surface current distribution, radiation patterns in both 2D and 3D, and the gain performance across the operating band. These outputs validate the designed geometry and confirm whether the antenna meets the expected behavior at 38 GHz.

3.1 Return Loss (S11) and Gain

Figure 3.1 shows the simulated return loss of the designed antenna. The antenna exhibits a clear resonance at 38 GHz, where the S11 value reaches approximately -16.088 dB, indicating acceptable impedance matching at the target frequency. The curve also demonstrates that the antenna maintains its performance within a narrow range around the operating frequency, which is typical for thin-wire Yagi structures. Figure 3.2 shows the simulated gain of Yagi–Uda antenna.

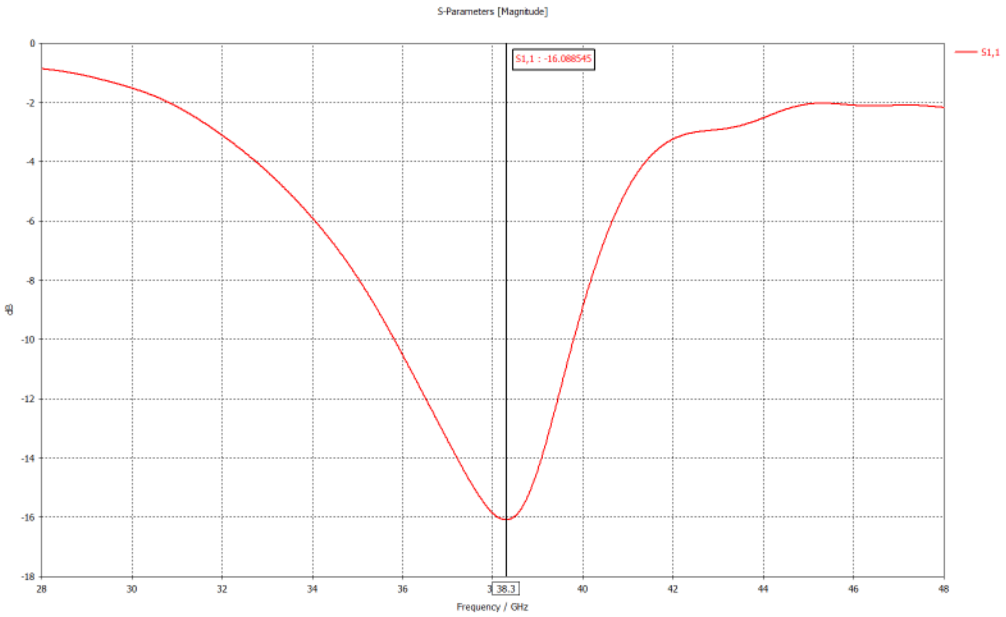

Figure 3.1: Simulated return loss (S11) of the Yagi–Uda antenna.

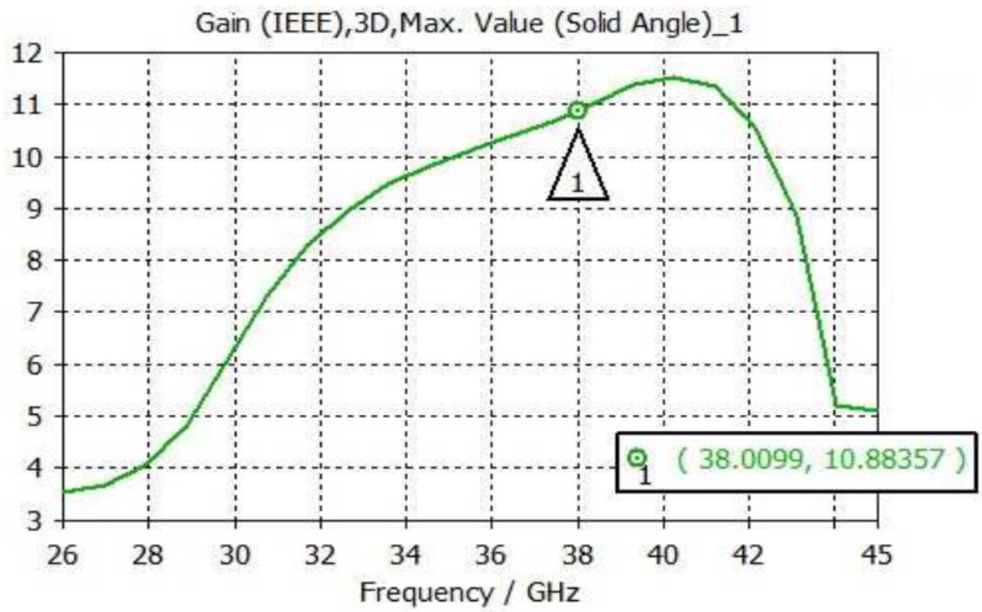

Figure 3.2: Simulated Gain of the Yagi–Uda antenna.

3.2 Surface Current Distribution

Figure 3.3 shows the surface current distribution of the antenna at 38 GHz. As expected, the driven element exhibits the highest current density, while the reflector and directors support progressively weaker induced currents. The current gradually decreases along the director chain, confirming the end-fire operation of the Yagi–Uda antenna and validating the intended coupling behavior between elements.

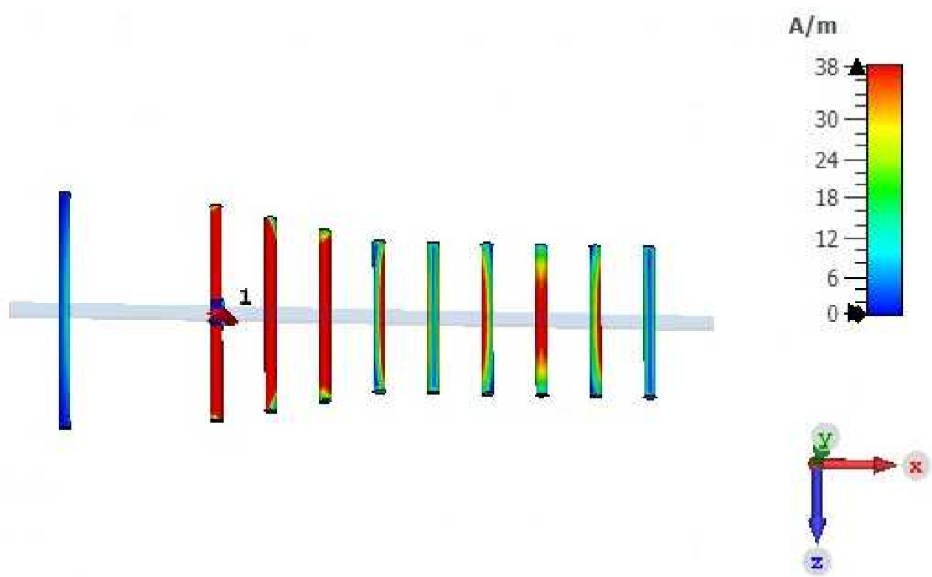

Figure 3.3: Surface current distribution at 38 GHz.

3.3 Radiation Pattern Analysis

The radiation behavior of the designed Yagi–Uda antenna was evaluated using 2D polar cuts and 3D far-field patterns at 38 GHz. Both linear and logarithmic (dB) scales are presented to illustrate the main-lobe direction, beamwidth, and relative sidelobe levels.

3.3.1 2D Radiation Patterns

The 2D polar cuts (E/H planes) show a clear end-fire main lobe with a peak magnitude of approximately 10.8 dBi. The half-power beamwidth (HPBW) measured from the primary cut is about 52° (see Figures 3.4 and 3.5). These results confirm that the designed Yagi–Uda geometry produces a narrow, high-gain main lobe at the target frequency and that the linear and logarithmic views are consistent in identifying the main-beam direction and angular width.

Theta Cuts ($\theta = 0°$ and $\theta = 90°$)

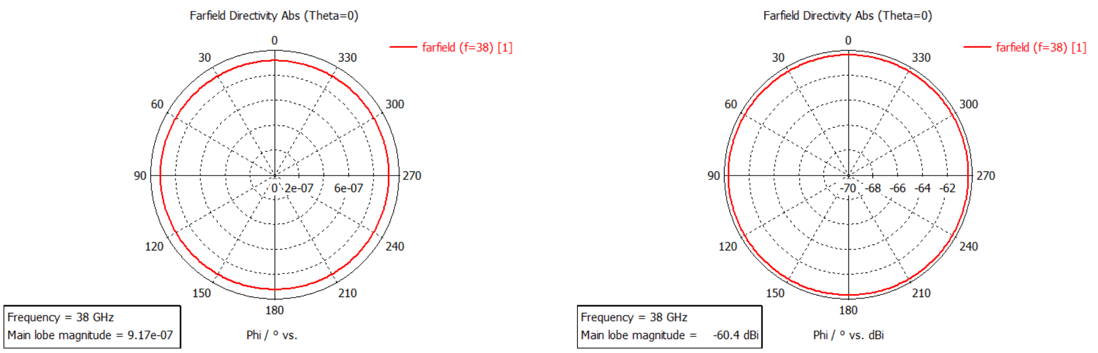

(a) Linear scale (b) Logarithmic scale

Figure 3.4: Radiation pattern for $\theta = 0°$.

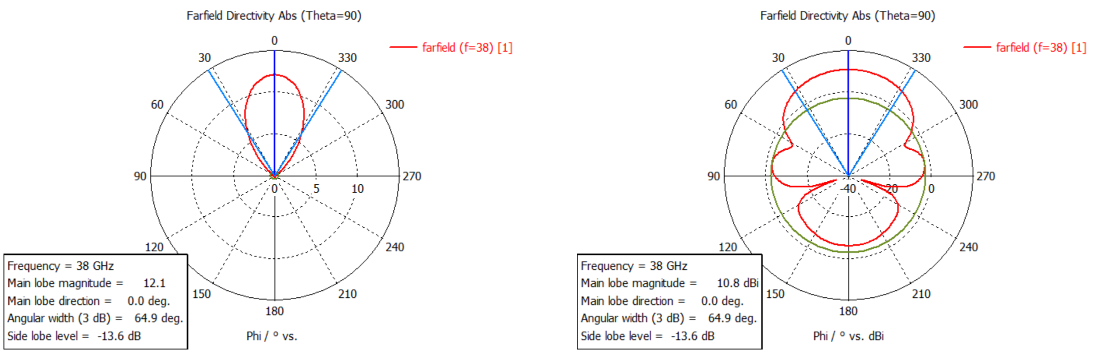

(a) Linear scale (b) Logarithmic scale

Figure 3.5: Radiation pattern for $\theta = 90°$.

Phi Cuts ($\phi = 0°$ and $\phi = 90°$)

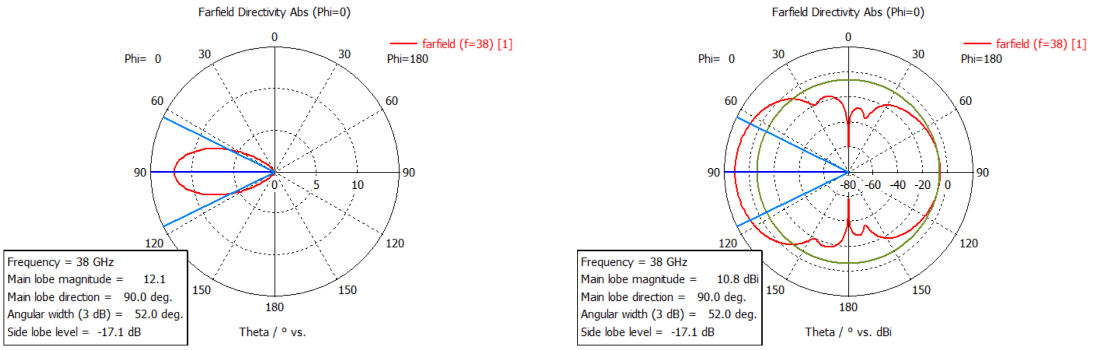

(a) Linear scale (b) Logarithmic scale

Figure 3.6: Radiation pattern for $\phi = 0°$.

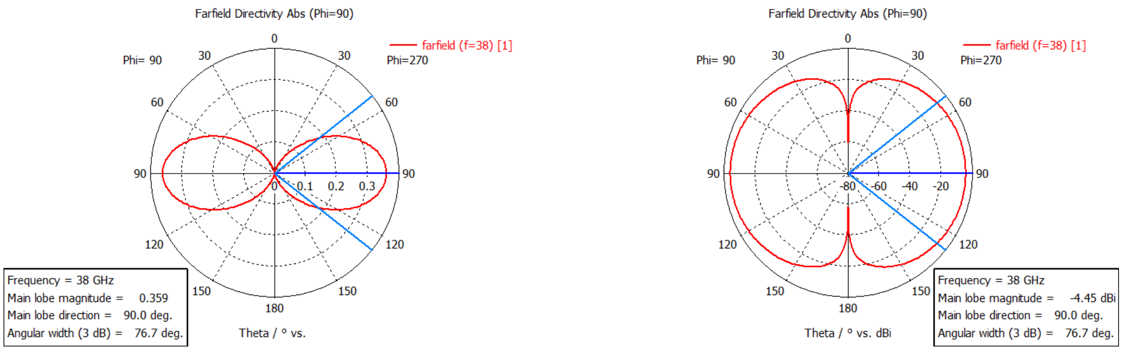

(a) Linear scale (b) Logarithmic scale

Figure 3.7: Radiation pattern for $\phi = 90°$.

3.3.2 3D Radiation Patterns

The 3D far-field renderings corroborate the 2D observations: the antenna exhibits end-fire radiation directed along the intended axis with a peak gain of 10.8 dBi and an overall beamwidth comparable to the 2D HPBW (52°). The linear 3D plot highlights the main-lobe shape with 97.45% efficiency, while the logarithmic view emphasizes sidelobe suppression, together confirming the focused forward radiation and good agreement with the design intent (see Figures 3.8 and 3.9).

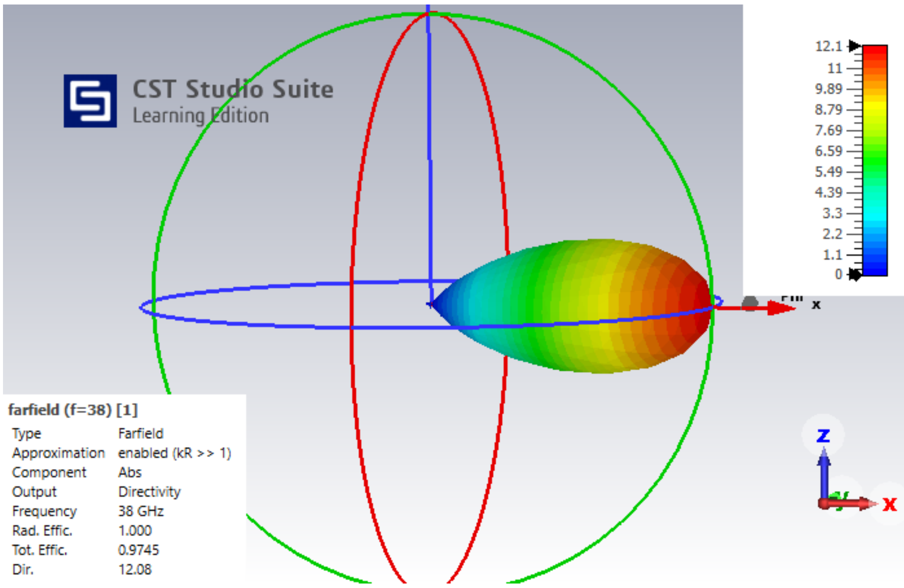

Figure 3.8: 3D radiation pattern at 38 GHz (linear scale).

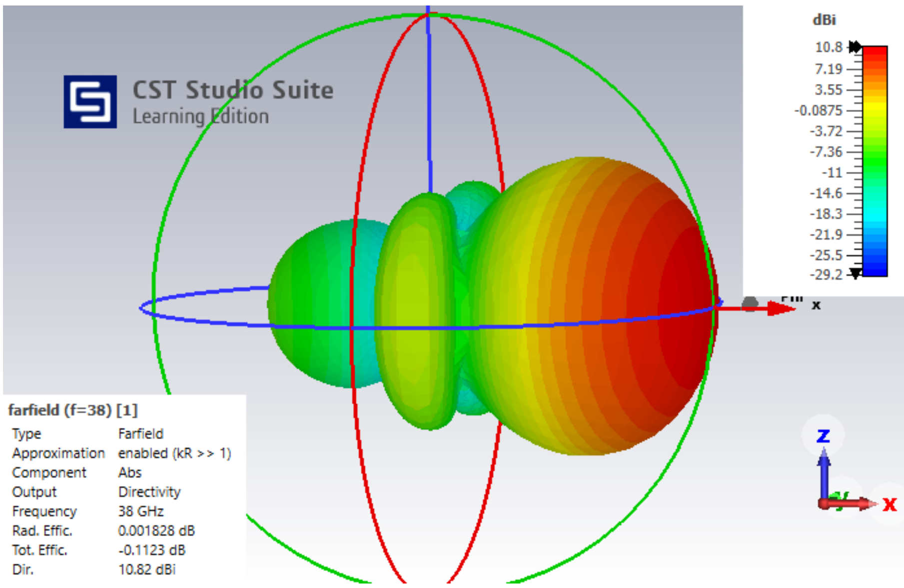

Figure 3.9: 3D radiation pattern at 38 GHz (logarithmic scale).

4 Conclusion

The 10-element Yagi–Uda antenna was successfully designed and simulated at 38 GHz using CST Studio Suite, following the geometry and guidelines provided in the reference work. The simulated structure achieved a return loss of approximately -16.088 dB at the target frequency, confirming good impedance matching. The radiation characteristics indicated clear end-fire behavior, with a measured peak gain of about 10.8 dBi and a half-power beamwidth of nearly $52°$, consistent with the expected performance of a millimeter-wave Yagi configuration. The 2D and 3D radiation patterns verified strong forward radiation and minimal back radiation, demonstrating correct coupling between the reflector, driven element, and director array.

To assess the similarity between the implemented design and the reference work, a comparison of key antenna parameters is presented in Table 4.1. The close agreement between the two sets of results confirms that the simulated model accurately reproduces the expected behavior of the reference Yagi–Uda antenna.

Table 4.1: Comparison of Simulated Results with Reference Paper

Parameter	**Reference Paper**	**This Work**
Operating Frequency (GHz)	38	38
Return Loss S11 (dB)	-16.29	-16.088
Peak Gain (dBi)	10.88	10.8
Half-Power Beamwidth (°)	51.7	52
Radiation Efficiency (%)	99	97.45